Weak nanoscale chaos and anomalous relaxation in DNA

Alexey K. Mazur

UPR9080 CNRS, Université Paris Diderot, Sorbonne Paris Cité, Institut de Biologie Physico-Chimique,
13, rue Pierre et Marie Curie, Paris, 75005, France

Anomalous nonexponential relaxation in hydrated biomolecules is commonly attributed to the complexity of the free-energy landscapes, similarly to polymers and glasses. It was found recently that the hydrogen-bond breathing of terminal DNA base pairs exhibits a slow power-law relaxation attributable to weak Hamiltonian chaos, with parameters similar to experimental data. Here, the relationship is studied between this motion and spectroscopic signals measured in DNA with a small molecular photoprobe inserted into the base-pair stack. To this end, the earlier computational approach in combination with an analytical theory is applied to the experimental DNA fragment. It is found that the intensity of breathing dynamics is strongly increased in the internal base pairs that flank the photoprobe, with anomalous relaxation quantitatively close to that in terminal base pairs. A physical mechanism is proposed to explain the coupling between the relaxation of base-pair breathing and the experimental response signal. It is concluded that the algebraic relaxation observed experimentally is very likely a manifestation of weakly chaotic dynamics of hydrogen-bond breathing in the base pairs stacked to the photoprobe and that the weak nanoscale chaos can represent an ubiquitous hidden source of nonexponential relaxation in ultrafast spectroscopy.

In physics, slow nonexponential relaxation is considered as a hallmark of complexity of condensed disordered systems, notably, polymers, glasses, and supercooled liquids. Such kinetics is called anomalous and it results from dynamics on complex energy landscapes with many coupled degrees of freedom [1]. The same interpretation is commonly applied to anomalous relaxation in hydrated proteins [2–4] and double helical DNA [5,6]. We found recently that the hydrogen-bond (HB) breathing of terminal DNA base pairs exhibits a slow power-law relaxation attributable to weak Hamiltonian chaos [7]. Its parameters appeared similar to the experimental data obtained by time-resolved fluorescence Stokes shift (TRFSS) spectroscopy [6]. Since the fluorescent probes are never placed near DNA ends the specific motion we studied could not play a role in earlier experiments and, strictly speaking, the above agreement was accidental. Nevertheless, the standard qualitative interpretation of these experimental data is very controversial and there are reasons to believe that localized weakly chaotic modes represent the true physical cause of anomalous relaxation in hydrated biomolecules where this phenomenon was revealed by small molecular probes [7].

Power-law distributions are ubiquitous in physics because this law is a large number limit for sums of random variables with infinite variances [8–10], that is, it plays a universal role similar to that of the Gaussian. Therefore, when two processes share a power-law form of time autocorrelation functions, it just means that both processes involve substates with broad lifetime distributions, but not necessarily coupled. The similarity of exponents is a stronger evidence, but these values are estimated with limited accuracy, whereas they are not very different between many distinct processes. For a casual relationship between the base-pair breathing and the TRFSS data, this motion should occur in a close vicinity of the photoprobe and this dynamics should modulate a strong applied electrostatic field. Both of these conditions are problematic. The opening of internal DNA base pair should be

negligible under relatively low temperatures used in TRFSS experiments (15°C, [5]). Besides, dynamics of internal base pairs is strongly restricted and its parameters can differ from those we obtained for terminal bases [7]. The origin of the strong electrostatic field modulated by base-pair breathing is also unclear. To shed light upon the above problems here the base-pair breathing is studied in an experimental DNA fragment by combining the earlier computational approach [7] with a new analytical theory. The intensity and the slow relaxation of these dynamics are studied in the internal base pairs that flank the coumarin photoprobe. An alternative mechanism of coupling between these motions and the TRFSS response signal is proposed.

The model system is designed as shown in Fig. 1. A DNA duplex is placed in a periodic box with 456 water molecules and eight sodium ions. The sequence of this DNA is $\frac{GCMCG}{CG\_GC}$, where M stands for coumarin. In Fig. 1(b) the duplex is shown from the major groove side; the opposite groove is called minor. This molecule is a representative fragment of the experimental DNA [5,6]. The photoprobe (coumarin C102) is inserted into the middle of the stack formed by four base pairs, with two oxygens exposed into the major groove. This photoprobe has approximately the size of a base pair and it is not exactly planar. The DNA end fraying was prevented by flat-bottom restraints applied to hydrogen bonds in the terminal base pairs. All-atom MD simulations were carried out as described earlier [7]. Other details can be found in Appendix A.

The HB breathing was followed by measuring the statistics of Poincaré recurrences for distances (R) between atoms that form Watson-Crick (WC) H bonds. The celebrated Poincaré recurrence theorem of 1890 [11] guarantees that a dynamic trajectory with a fixed energy and bounded phase space will always return in a close vicinity of the initial state. The statistics of recurrences is defined as the probability distribution $P(\tau)$ of returns with times longer than τ. Hamiltonian dynamics can be regular and chaotic [12]. In purely chaotic phase spaces,
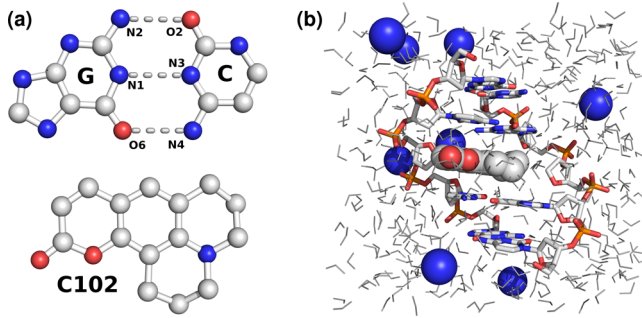
FIG. 1. (a) The stack components: a GC base pair, with three H bonds indicated by thick dashed lines (top), and a coumarin C102 residue (bottom), both shown with the major groove edges facing down. (b) The model system used in MD simulations. The DNA structure is shown by sticks and the hydration water is displayed by thin lines. The coumarin residue and the sodium ions are highlighted by spheres. The standard DNA atom color coding is used, that is, gray, red, blue, and orange for carbons, oxygens, nitrogens, and phosphates, respectively.

any trajectory rapidly fills accessible areas and $P(\tau)$ drops exponentially, like the probability of any region to remain unvisited during time τ [13,14]. In contrast, in mixed phase spaces where islands of stable regular motion are embedded in a chaotic sea $P(\tau)$ decays as [15,16]

$$P(\tau) \propto 1/\tau^{\beta}. \qquad (1)$$

This occurs because the stability islands are commonly covered by boundary layers of fractal structures formed by smaller islands, and chaotic trajectories are trapped in these layers for very long periods [17]. This complexity is intrinsic in Hamiltonian systems of any size. The power-law decay is persistent in canonical models with one or several degrees of freedom [18–22]. For canonical model systems, the Poincaré exponent is $\beta \sim 1.5$ [15,16,23–26], but in real dynamics it may vary with the interaction potential [7]. Probably the simplest mechanical example is the three-body Coulomb problem [27]. In large heterogeneous systems like hydrated macromolecules the algebraic decay is overshadowed by numerous chaotic modes, but it can manifest itself in special conditions [7].

In DNA dynamics, the stopwatch is started when a given distance exceeded a certain threshold (R_{th}) and stopped once the boundary is crossed in the opposite direction. $P(\tau)$ is obtained by counting the number of recurrences with duration larger than τ and normalizing it by the total number of events, that is, $P(0) = 1$ by construction. The fraction of time spent in the opened state is evaluated simultaneously. These computations are trivially parallelizable, that is, the $P(\tau)$ statistics can be accumulated in a large number of independent MD trajectories. The results discussed below were obtained by using parallel computations on 129 cores for a model system with 3557 degrees of freedom for 1665 atoms to obtain the total sampling of about 100 μs.

Table I contains populations of partially opened states of GC pairs in different locations. These populations were measured in MD as fractions of trajectory time spent with $R > R_{th} = 4.15$ Å for the three H bonds indicated in Fig. 1(a). The probability of opening strongly depends upon the H bond

TABLE I. Populations (in ppm) of opened HB states for different GC base pairs. The internal and terminal base pairs in unmodified tetramer DNA [7] are coded as I and T, respectively. The two pairs stacked to the photoprobe are denoted according to the DNA strand direction, that is, 5′n (5′-neighbor, upper in Fig. 1(b)) and 3′n (lower), respectively.

HB	I	T	5′n	3′n
O6-N4	9	1043	22	7868
N1-N3	0	197	7	5033
N2-O2	1	46	3	12005

as well as the environment of the base pair. In unmodified DNA the internal base pairs are very stable compared to the terminal ones; the O6-N4 H bonds are opened easier than others and the breathing predominantly occurs toward the major groove, that is, toward the viewer in Fig. 1(b). The HB breathing in internal pairs is strongly increased when they are stacked to the intercalated coumarin. From the 5′ side of the photoprobe this increase is moderate, but the opposite 3′n pair is perturbed very strongly. The HB breathing in this GC pair qualitatively differs from others because the N2-O2 and O6-N4 H bonds appear more labile than the central one, which means that partial openings occur toward both grooves.

Figure 2(a) displays the statistics of recurrences to threshold $R_{th} = 3.15$ Å for a few representative H bonds. For internal base pairs the $P(\tau)$ profile is nearly exponential until $\tau \approx 1$ ps. The exponential regime is similar for all H bonds. It results from rapid chaotic oscillations within bonded ground states because the saddle point of the H bond potential occurs well beyond 3.15 Å. Slower returns to R_{th} are due to trajectories that wander outside the ground-state valley and they give an algebraic decay of $P(\tau)$. As shown in Fig. 2(b) the relative weight of slow returns naturally grows with R_{th}. An example of a partially opened structure is shown in Fig. 3. It is seen that in the upper base pair the hydrogen bond at the major groove side is broken by a stable bridging water molecule in direct contact with coumarin.
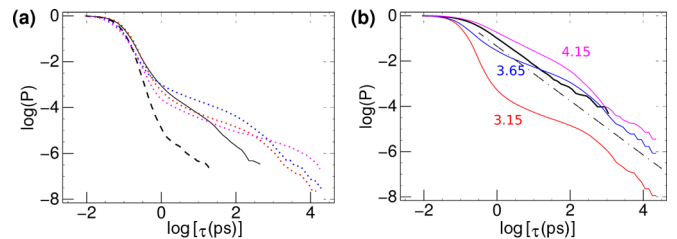

FIG. 2. (a) The statistics of Poincaré recurrences $P(\tau)$ for five WC H bonds ($R_{th} = 3.15$ Å). The black solid and dashed lines correspond to O6-N4 bonds in terminal and internal base pairs, respectively, in unmodified DNA [7]. The colored dotted traces correspond to the three H bonds of the 3′n pair in Table I. (b) $P(\tau)$ profiles corresponding to the O6-N4 bond of the 3′n pair computed for three different thresholds R_{th} indicated in the figure. The solid black line shows the corresponding trace for terminal base pairs in unmodified DNA ($R_{th} = 4.15$ Å). The dash-dotted straight line shows the power-law decay with the exponent $\beta = 1.2$. The logarithms are decimal.
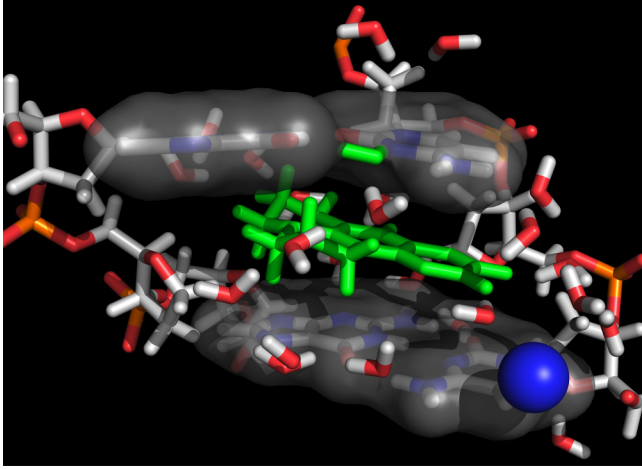
FIG. 3. A snapshot from MD simulation of the model DNA fragment with a partially opened base pair stacked to coumarin. The coumarin residue in the middle of the plate is highlighted by green. It is seen that the O6-N4 hydrogen bond in the upper GC pair is broken and replaced by a bridging water molecule highlighted similarly to coumarin. Other water molecules shown and the sodium ion (blue sphere) take part in the coumarins hydration shell in the major groove.

Such structures become possible when the hydrogen bond is stretched by more than one angstrom, i.e., to the length of about 4 Å. As seen in Fig. 2(b), this distance is the threshold beyond which the exponential relaxation becomes negligible.

The transition between the exponential and algebraic regimes depends upon the H bond and the base-pair location, but eventually the power-law decay Eq. (1) is established with an exponent close to $\beta = 1.2$ obtained for end fraying [7]. This is shown in Fig. 2 and Fig. 4(a), respectively, for 3′n and 5′n pairs from Table I. At the same time, the HB breathing in the coumarin's neighbors cannot be similar to the fraying of terminal base pairs, and it evidently differs, which is seen in the shapes of the plots in Fig. 2 and the relative populations of open states in Table I. In addition, Fig. 4(b) shows that the end fraying is accompanied by a faster growth of the average distance between the reference atoms with the life time of the opened state. These results argue against the mechanisms
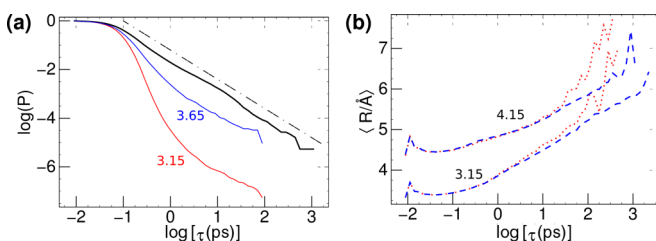

FIG. 4. (a) $P(\tau)$ profiles corresponding to the O6-N4 bond of the 5′n pair in Table I computed for two thresholds R_{th} indicated in the figure. The solid black line shows a similar trace for terminal base pairs in unmodified DNA ($R_{\text{th}} = 3.55$ Å). The dash-dotted straight line shows the power-law decay with the exponent $\beta = 1.2$. (b) The dependencies of average distances $\langle R \rangle$ for O6-N4 H bonds in the 3′n pair (dashed blue) and terminal base pairs (dotted red) for two thresholds indicated in the figure. The logarithms are decimal.

of the fractional Brownian motion [28] in the dynamics of HB-distances and the corresponding stochastic origin of the power-law decay. Such models would produce the growth $\langle R \rangle \propto \tau^H$, with the Hurst index H defining the exponent β in Eq. (1). In contrast, Fig. 4(b) reveals that this growth is nearly linear in semilogarithmic coordinates. Moreover, the value of β is robust against the differences in the growth rates, which agrees with the suggestion based upon the chaos theory that β is determined by the degree of the polynomial that approximates the energy profile near the saddle points [7]. This parameter should not depend upon the base pair location.

The power-law relaxation in DNA has been revealed by TRFSS in a broad time range starting from subpicoseconds [5,6]. This phenomenon was analyzed with different theories [29–32], but its origin remains controversial. The DNA double helix has only a few well-studied conformational substates with spatially localized dynamics that poorly fits the energy landscape description. There are slow modes in the conformational dynamics of coumarin and DNA, but the possible candidates [32] involve only one or a few local minima and they cannot result in broad lifetime distributions. In contrast, the hydration dynamics can be complex, but it does not have relaxation modes beyond the picosecond range [33,34]. At present, there is no agreement even on whether this effect is due to DNA itself, or the hydration water, or both [33–35].

The optical $S0 \rightarrow S1$ transition in coumarins instantaneously increases the dye's dipole moment and perturbs the electrostatic equilibrium of its environment [36]. The Stokes effect occurs due to re-equilibration the environment during the excitation lifetime and results in a fluorescence red shift. The four bases stacked to the photoprobe in DNA represent the major part of its environment, therefore, the HB breathing and the fluorescence transitions are likely to be coupled. However, a causal relationship between the HB breathing and the power-law relaxation revealed in experiments is not at all evident. The measured signal is

$$S(t) = \frac{\nu(t) - \nu(\infty)}{\nu(0) - \nu(\infty)}, \tag{2}$$

where $\nu(t)$ is the fluorescence emission frequency and t is the time after laser excitation. For theoretical analysis, $S(t)$ is commonly approximated as

$$S(t) \approx C(t) = \frac{\langle \delta E(0) \delta E(t) \rangle}{\langle \delta E(0)^2 \rangle}, \tag{3}$$

where $E(t)$ and $C(t)$ represent the solvation energy and its equilibrium autocorrelation function, respectively. This splits the experimental response into a sum of autocorrelation functions of independent electrostatic contributions. To account for the experimental data this sum must involve a power-law term with an exponent around 0.15 [6]. A similar value is obtained from Eq. (1) with $\beta = 1.2$ by using an estimate proposed in the chaos theory [23,25],

$$C(\tau) \propto \tau P(\tau), \tag{4}$$

but this is just a curious mathematical coincidence (see Appendix B). Indeed, the power spectral density of time fluctuations for HB distances considered here decays with an

exponent $\eta = 1.63$ [7], which means that in Eq. (3) the effect of a hypothetical electrostatic field modulated by the base-pair breathing would disagree with the available experimental data.

The physical coupling between the measured TRFSS signal and the base-pair breathing can have a completely different origin. This alternative mechanism is described below. Although the effect is nonlinear and complex, its physics is similar to that in a simple two-state system described by linear kinetics. In the most relevant case, when the lifetime of the opened base-pair state is very small, a general solution is also available. The following derivations employ a perturbative approach in the sense that the qualitative similarity with linear system is used as long as possible, with the main result derived by applying the same ideas in the principal limiting case. The general solution for the linear system and the underlying assumptions are discussed in larger detail in Appendix C.

A photoprobe can receive a photon when the neighboring base pairs are closed (A) or partially opened (B). The excited coumarins are partitioned between the two states with concentrations C_A and C_B, respectively. In the linear approximation the balance between them is described by schema

$$0 \xleftarrow{k_0} A \underset{k_-}{\overset{k_+}{\rightleftharpoons}} B \xrightarrow{k_0} 0, \tag{5}$$
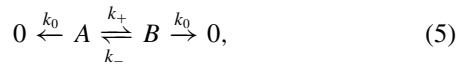
where k_+ and k_- are the rate constants of base-pair opening and closing, respectively, and the quenching constant k_0 determines the excitation lifetime. In states A and B, the solvent relaxation and the red-shifted emission occur according to the conventional scenario described by Eqs. (2) and (3); however, the fluorescence parameters in these two states can differ. The excitation and emission spectra of coumarin in water are significantly shifted from those in DNA, and the excitation lifetime is much shorter [37]. Similar changes are observed when DNA samples with intercalated coumarins are melted [37]. In state B, new water molecules like that in Fig. 3 come in between the bases and, due to their high polarity and direct contact with coumarin, they can alter the fluorescence parameters.

Let $f = C_B/(C_A + C_B)$ denote the relative population of opened pairs stacked to excited coumarins. The observed emission frequency $v(t)$ in Eq. (2) is

$$v = (1 - f)v_A + f v_B = v_A + f(v_B - v_A), \tag{6}$$

where v_A and v_B are the emission frequencies of the two states, respectively. Because the static spectral shift $v_B - v_A$ is large compared to the maximal amplitude of the time-dependent response [37], even a small time variation of $f(t)$ can be noticeable. Assuming that the solvent relaxation is fast and v_A and v_B always remain at steady state levels, Eq. (2) gives

$$S(t) = \frac{f(t) - f(\infty)}{f(0) - f(\infty)}. \tag{7}$$

In the linear case, the relaxation to equilibrium is exponential,

$$f(t) = f(\infty) + \delta \exp(-\lambda t), \tag{8}$$

$$S(t) = \exp(-\lambda t), \tag{9}$$

where $\lambda = k_+ + k_-$ is the only nonzero eigenvalue and δ is the initial perturbation (see Appendix C). The $S0 \rightarrow S1$ excitation due to the laser pulse changes the eigenvalues and creates a population of base pairs stacked to excited coumarins with a perturbed $A \rightleftharpoons B$ equilibrium, which causes a TRFSS response.

Now consider a nonlinear case when the $B \rightarrow A$ transition gives a nonexponential statistics of Poincaré recurrences $P(\tau)$, which means that it is not a Markov process, and the probability of base-pair closing effectively depends upon the time spent in the open state (trapping time). When the system is in detailed balance equilibrium the $A \rightarrow B$ and $B \rightarrow A$ flows are mutually compensated due to steady-state trapping time distributions established for both opened and closed pairs. With stationary distributions, the flows are proportional to concentrations, which makes the problem equivalent to the linear case. The shapes of the stationary distributions are similar in base pairs stacked to normal and optically excited coumarins. For instance, if the coumarin excitation lifetime is smaller in state B this sub-population will disappear more rapidly, but the trapping time distribution is not affected because the rate of quenching does not depend upon the previous history of the opened pair.

When the laser pulse arrives at $t = 0$, the initial state of the subpopulation of base pairs stacked to excited coumarins can be decomposed into a constant part corresponding to the new equilibrium, and a perturbation which disappears in the course of relaxation. The irreversible decay of this second part corresponds to the TRFSS signal that we want to evaluate. At $t = 0$ both parts have the stationary trapping time distributions established before the excitation. With $t > 0$, the assumption of stationarity remains valid for the first part, but for the irreversible decay of the perturbation this assumption fails, therefore, the equivalence with the linear problem is lost. However, when the lifetime of state B is small compared to that that of state A the kinetics of decay is entirely determined by the starting trapping time distribution in B, and the analytical solution exists in the general case.

The main idea can be understood from the linear case. The perturbation is an antisymmetric vector in the space of concentrations (C_A, C_B), because it represents an excess in one state and an equal deficit in the other with respect to the equilibrium. Suppose $\delta > 0$ in Eq. (8), i.e., the equilibrium is perturbed by transferring a small number of molecules from A to B. Since $k_- \gg k_+$, this does not change the $A \rightarrow B$ flow and increases the $B \rightarrow A$ flow by the rate of decay of the excess in B. With $\delta < 0$ the excess is created in A and the deficit in B. The $A \rightarrow B$ flow is again changed negligibly, but the opposite flow is strongly reduced and the corresponding part of the equilibrium $A \rightarrow B$ flow is not compensated. As a result, the deficit in B is reduced with the same rate as the excess the previous case, and the relaxation always looks like a decay of the state with the smaller lifetime.

Now consider the general case. With $\delta > 0$ at time $t = 0$ we have an excess of opened pairs with a stationary trapping time distribution. In equilibrium, base pairs are opened with a constant rate v. The stationary distribution is the probability density of pairs opened already for time τ, that is

$$\int_\tau^\infty p(t) v \, dt = v P(\tau), \tag{10}$$

where $p(t)$ is the normalized probability density of Poincaré returns,

$$\int_0^\infty p(t)dt = 1. \qquad (11)$$

Let $C_B(t)$ denote the number of opened pairs corresponding to the excess $\delta > 0$. We have

$$C_B^0(0) \propto \int_0^\infty P(\tau)d\tau. \qquad (12)$$

This perturbation evolves as if the opening of base pairs stopped at $t = 0$. The probability that a pair already opened for time τ will stay opened during time t is $P(\tau + t)$. Therefore, the initial perturbation $C_B^0(0)$ decays with time as

$$C_B(t) \propto \int_0^\infty P(\tau + t)d\tau = \int_t^\infty P(\tau)d\tau. \qquad (13)$$

Substitution into Eq. (7) yields the measured response function

$$S(t) \propto \int_t^\infty P(\tau)d\tau \qquad (14)$$

and Eq. (4) for power-law decays. Now consider the case $\delta < 0$. At time $t = 0$, we have a deficit in the equilibrium distribution of opened pairs, which is reduced by a constant flow from the equilibrated pool of closed pairs. The equilibrium will be reestablished when the deficit is closed, with the stationary trapping time distribution recovered. The time dependence is computed as

$$C_B(t) \propto \int_0^t P(\tau)d\tau = \text{const} - \int_t^\infty P(\tau)d\tau, \qquad (15)$$

and substitution into Eq. (7) again yields Eq. (14).

The above theory suggests that the power-law relaxation experimentally observed in DNA is indeed caused by the base-pair breathing dynamics. The equilibrium population of partially opened pairs is low, which means that the rate of base-pair closing is much larger than that of opening. Therefore, the decay of fluctuations is dominated by base-pair closing in agreement with the assumption used above. Although our model system has many degrees of freedom, the HB breathing is essentially a one-dimensional motion. The weak dynamic chaos is currently the only and the most reasonable explanation of the observed algebraic relaxation. It is difficult, however, to obtain a formal proof of this assertion because of a limited choice of instruments of the chaos theory applicable to large systems. Further work in this direction is necessary.

The theory developed above also clarifies an unclear issue concerning the role of the coumarin's dipole moment. Presentations of the TRFSS method often start from an assertion that optical $S0 \rightarrow S1$ transitions strongly increase the dye's dipole moments. This is necessary for slow relaxation in the conventional approach because a significant area around the dye must be involved and the long-range electrostatic interactions are indispensable [36]. However, for coumarin C102 shown in Fig. 1(a) the measured increase of the dipole moment does not exceed 40%, with absolute values between two and three debyes [38]. Quantum mechanics calculations show that the dipoles of $S0$ and $S1$ states as well as their difference are distributed over the whole molecule rather than localized, and MD simulations with excited coumarin reveal

no difference from the ground state (unpublished). Indeed, in an aqueous ionic environment a distributed dipole similar to that of a single water molecule can hardly cause noticeable long-range effects. The alternative mechanism proposed above resolves this controversy because it is applicable even with zero dipole moments.

In summary, it is shown that, in contrast to traditional statistical mechanics explanations, the power-law relaxation earlier discovered in DNA is likely to result from chaotic dynamics of a few or even one degree of freedom of HB breathing in the base pairs flanking the photoprobe. The new theory is generally applicable to ultrafast relaxation techniques, and it may be interesting to look for instances of weak nanoscale chaos in other controversial cases of algebraic relaxation in different systems.

APPENDIX A: MOLECULAR DYNAMICS SIMULATIONS

DNA duplexes were modeled in aqueous environment neutralized by sodium ions [39], using a recent version of the all-atom AMBER forcefield [40–43] with SPC/E water [44] in periodic boundaries. The coumarin partial charges were obtained by the RESP method [45,46], with sugar and phosphate charges corresponding to standard AMBER values. The electrostatic interactions were treated by the SPME method [47], with 9 Å truncation for the real space sum and common values of other Ewald parameters [48]. The temperature was maintained by the Berendsen algorithm [49] applied separately to solute and solvent with a relaxation time of 10 ps. The average temperature was about 298K. To increase the time step, MD simulations were carried out by the internal coordinate method (ICMD) [50,51], with the internal DNA mobility limited to essential degrees of freedom. The rotation of water molecules and internal DNA groups including only hydrogen atoms was slowed down by weighting of the corresponding inertia tensors [48,52]. The double-helical DNA was modeled with free backbone torsions and bond angles in sugar rings. Phosphate groups and aromatic cycles were rigid. The net effect of these constraints upon DNA dynamics is not significant, which was checked earlier through comparisons with conventional Cartesian MD [48,53]. The time step was 0.01 ps. The statistics of Poincaré recurrences $P(\tau)$ is a positive definite function stable with respect to fluctuations in contrast to time autocorrelation functions. Importantly, its numerical evaluation is trivially parallelizable, that is, it can be accumulated in a large number of independent MD trajectories. The results presented in the text were obtained by using parallel computations on 129 cores for the model system that had 3557 degrees of freedom for 1665 atoms to obtain the total sampling of about 100 μs.

In the modeled DNA duplex, the base pairs flanking the coumarin probe are next to the terminal ones that also can be opened. In such cases, the base pair under study is effectively transformed into a terminal one. In experiments, this duplex

is part of a longer DNA and we would like to simulate the corresponding environment. Moreover, for reliable statistical averaging stable conditions are required, that is, the dynamics should not involve slower motions that cannot be averaged during in the same trajectory. The base flipping of terminal base pairs can be discarded, for instance, by stopping the trajectory. A more practical solution consists in applying flat-bottom restraints to some hydrogen bonds in the external base pairs as explained elsewhere [54]. The restraints are switched off when the distance between the hydrogen bonded heavy atoms is below 3.8 Å, that is, they do not perturb DNA dynamics but increase the probability of closure when the hydrogen bond is opened. The internal base pairs were free to open completely. In three such cases one of the residues in the $3'n$ base pair flipped out and remained outside the stack. This did not affect the results, which was checked by excluding these three trajectories from the analysis. Other base pairs opened only temporarily, with all such events reversed at the end.

APPENDIX B: STATISTICS OF POINCARÉ RECURRENCES AND AUTOCORRELATION FUNCTION

In the chaos theory, the autocorrelation function $C(\tau)$ and the probability $P(\tau)$ are related as [23,25]

$$C(\tau) \propto \tau P(\tau). \tag{B1}$$

This relationship follows from the following reasoning. Suppose we have an indicator function $f(t)$ such that $f = 1$ on the intervals counted as Poincaré returns and $f = 0$ elsewhere. The unnormalized autocorrelation function is defined as

$$C(\tau) = \int_0^\infty f(t) f(t+\tau) dt. \tag{B2}$$

Nonzero contributions to this integral come from returns longer than τ. Duration $t > \tau$ gives a contribution $t - \tau$, while the number of such returns is $-dP(t)$; therefore,

$$C(\tau) = -\int_\tau^\infty (t - \tau) P_t' dt = -\int_\tau^\infty t P_t' dt + \int_\tau^\infty \tau P_t' dt.$$

Assuming that $P(\tau)$ is smooth and integrable, the above integrals readily result in

$$C(\tau) = \int_\tau^\infty P(t) dt \tag{B3}$$

and Eq. (B1) for the power-law decay.

The above derivation works for canonical chaotic systems [23,25], because trajectories are quasiperiodic during long stays near stability islands and chaotic in between them. Chaotic intervals do not contribute to Eq. (B2) and quasiperiodic motion gives contributions proportional to the lengths of intervals. Different quasiperiodic intervals are uncorrelated on average. For the distances measured in MD, these conditions are violated already because the averages grow with the duration of opening (see Fig. 3). The power spectral density of time dependencies decays with a power-law exponent $\tau = 1.63$ [7], which means that the corresponding autocorrelation function cannot agree with Eq. (B1) under simple assumptions about the dimensionality of the space. This problem can be obviated by assuming that the electrostatic energy term that links the HB breathing with the dye's dipole momentum

is proportional to an indicator function incremented by ± 1 when the H bond is broken and reformed, respectively. The corresponding autocorrelation function should have a power-law tail with the desired exponent. However, this is an *ad hoc* mathematical rewording of the theory considered in the main text rather than a physical model compatible with Eq. (3). The agreement with experiment obtained in this way has no physical meaning.

APPENDIX C: LINEAR APPROXIMATION AND EXPONENTIAL RELAXATION

In the linear case, the dynamics of the subset of excited coumarins is described by schema

$$0 \xleftarrow{k_0} A \underset{k_-}{\overset{k_+}{\rightleftharpoons}} B \xrightarrow{k_0} 0, \tag{C1}$$
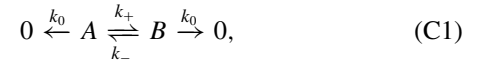
with the rate constants of base pair opening k_+ and k_-, respectively. Constant k_0 describes quenching due to any process and defines the excitation lifetime. The corresponding exponential decay is subtracted during the data processing and does not contribute to the response function $S(t)$. To discard it, the solution is written as $\mathbf{C}(t)\exp(-k_0 t)$, where vector $\mathbf{C}(t)$ corresponds to a simpler system, $A \underset{k_-}{\overset{k_+}{\rightleftharpoons}} B$, described by equation

$$\dot{\mathbf{C}} = \mathbf{M}\mathbf{C}; \quad \mathbf{C} = \begin{pmatrix} C_A \\ C_B \end{pmatrix}, \quad \mathbf{M} = \begin{pmatrix} -k_+ & k_- \\ k_+ & -k_- \end{pmatrix}, \tag{C2}$$

where C_A and C_B are relative populations of states A and B, respectively, while the overdot denotes time derivative. The general solution of Eq. (C2) is

$$\mathbf{C} = C_1 \mathbf{e}_1 \exp(-\lambda_1 t) + C_2 \mathbf{e}_2 \exp(-\lambda_2 t), \tag{C3}$$

with free constants $C_{1,2}$. The two eigenvalues and unnormalized eigenvectors computed as

$$\lambda_1 = 0, \quad \mathbf{e}_1 = \begin{pmatrix} k_- \\ k_+ \end{pmatrix}; \quad \lambda_2 = k_+ + k_-, \quad \mathbf{e}_2 = \begin{pmatrix} -1 \\ +1 \end{pmatrix} \tag{C4}$$

correspond to equilibrium and relaxation, respectively. Substitution of Eq. (C3) into Eq. (6) yields

$$S(t) = \exp(-\lambda_2 t). \tag{C5}$$

The exponential decay in Eq. (C5) looks irreversible because vector $\mathbf{e}_2$ is antisymmetric, which corresponds to an excess in B and a hole in A or vice versa. The hole is gradually closed without creating an opposite flow. If $k_- \gg k_+$ than $\lambda_2 = k_-$, that is, even if the perturbation is made by adding molecules to A the relaxation looks like a faster $B \to A$ transition. In this case the hole in B is closed by the equilibrium $A \to B$ flow, which is strong because $C_A^0 \gg C_B^0$ according to vector $\mathbf{e}_1$.

With different emission spectra in states A and B, a small difference in the excitation lifetimes is sufficient to cause a TRFSS response. This mechanism is applicable even if the coumarin's dipole moment is not changed by excitation. However, a large increase of the dipole moment characteristic for coumarins can perturb the $A \rightleftharpoons B$ equilibrium directly, which gives an alternative physically distinct perturbation pathway. The mathematical treatments of these two pathways are similar.

Suppose that the $S0 \rightarrow S1$ excitation in coumarin shifts the equilibrium, i.e., alters constants k_+ and/or k_-. When the laser pulse arrives, the system's eigenvalues and eigenvectors are changed instantaneously, which starts the relaxation to a new equilibrium described by an exponential decay with new (primed) $\mathbf{e}'_1$ and λ'_2,

$$\mathbf{C} = C^0 \mathbf{e}'_1 + \delta\mathbf{e}_2 \exp(-\lambda'_2 t), \tag{C6}$$

where C^0 and δ the components of the initial state in the primed basis. The same result is obtained if the excitation lifetimes in states A and B are slightly different. Suppose the quenching rates in states A and B are k_0 and $k_0 + \widetilde{k}$, respectively, with $\widetilde{k} \gtrapprox 0$. Matrix $\mathbf{M}$ in Eq. (C2) takes the form

$$\mathbf{M} = \begin{pmatrix} -k_+ & k_- \\ k_+ & -(k_- + \widetilde{k}) \end{pmatrix}, \tag{C7}$$

with slightly different eigenvalues and eigenvectors. As in the previous case after the laser pulse the $A \rightleftharpoons B$ dynamics in the subset of excited coumarins is out of equilibrium and the relaxation occurs according to Eq. (C6).

[1] J. Klafter and M. F. Shlesinger, Proc. Natl. Acad. Sci. USA **83**, 848 (1986).

[2] I. E. T. Iben, D. Braunstein, W. Doster, H. Frauenfelder, M. K. Hong, J. B. Johnson, S. Luck, P. Ormos, A. Schulte, P. J. Steinbach *et al.*, Phys. Rev. Lett. **62**, 1916 (1989).

[3] H. Frauenfelder, S. G. Sligar, and P. G. Wolynes, Science **254**, 1598 (1991).

[4] P. W. Fenimore, H. Frauenfelder, B. H. McMahon, and R. D. Young, Physica A **351**, 1 (2005).

[5] E. B. Brauns, M. L. Madaras, R. S. Coleman, C. J. Murphy, and M. A. Berg, Phys. Rev. Lett. **88**, 158101 (2002).

[6] D. Andreatta, J. L. P. Lustres, S. A. Kovalenko, N. P. Ernsting, C. J. Murphy, R. S. Coleman, and M. A. Berg, J. Am. Chem. Soc. **127**, 7270 (2005).

[7] A. K. Mazur and D. L. Shepelyansky, Phys. Rev. Lett. **115**, 188104 (2015).

[8] M. F. Shlesinger, G. M. Zaslavsky, and J. Klafter, Nature **363**, 31 (1993).

[9] J. Klafter, M. F. Shlesinger, and G. Zumofen, Phys. Today **49**(2), 33 (1996).

[10] I. Eliazar and J. Klafter, Phys. Rep. **511**, 143 (2012).

[11] H. Poincaré, Acta Math. **13**, 46 (1890).

[12] A. J. Lichtenberg and M. A. Lieberman, *Regular and Chaotic Dynamics* (Springer-Verlag, New York, 1992).

[13] V. I. Arnold and A. Avez, *Ergodic Problems of Classical Mechanics* (Benjamin, Paris, 1968).

[14] I. P. Cornfeld, S. V. Fomin, and Y. G. Sinai, *Ergodic Theory* (Springer, New York, 1982).

[15] B. V. Chirikov and D. L. Shepelyansky, in *Proceedings of the IXth International Conference on Nonlinear Oscillations, Kiev, 1981*, edited by Y. A. Mitropolsky (Nauk. Dumka, Kiev, 1984), pp. 421–424.

[16] B. V. Chirikov and D. L. Shepelyansky, Physica D **13**, 395 (1984).

[17] G. M. Zaslavsky, Phys. Today **52**(8), 39 (1999).

[18] M. Ding, T. Bountis, and E. Ott, Phys. Lett. A **151**, 395 (1990).

[19] A. J. Fendrik and M. J. Sanchez, Phys. Rev. E **51**, 2996 (1995).

[20] E. G. Altmann and H. Kantz, Europhys. Lett. **78**, 10008 (2007).

[21] D. L. Shepelyansky, Phys. Rev. E **82**, 055202(R) (2010).

[22] E. G. Altmann, J. S. E. Portela, and T. Tel, Rev. Mod. Phys. **85**, 869 (2013).

[23] C. F. F. Karney, Physica D **8**, 360 (1983).

[24] J. D. Meiss and E. Ott, Phys. Rev. Lett. **55**, 2741 (1985).

[25] B. V. Chirikov and D. L. Shepelyansky, Phys. Rev. Lett. **82**, 528 (1999).

[26] G. Cristadoro and R. Ketzmerick, Phys. Rev. Lett. **100**, 184101 (2008).

[27] P. Schlagheck and A. Buchleitner, Phys. Rev. A **63**, 024701 (2001).

[28] R. F. Voss, Phys. Rev. Lett. **68**, 3805 (1992).

[29] G. Kalosakas, K. O. Rasmussen, and A. R. Bishop, Chem. Phys. Lett. **432**, 291 (2006).

[30] S. Sen, D. Andreatta, S. Y. Ponomarev, D. L. Beveridge, and M. A. Berg, J. Am. Chem. Soc. **131**, 1724 (2009).

[31] N. Pal, S. D. Verma, and S. Sen, J. Am. Chem. Soc. **132**, 9277 (2010).

[32] K. E. Furse and S. A. Corcelli, J. Am. Chem. Soc. **133**, 720 (2011).

[33] B. Halle and L. Nilsson, J. Phys. Chem. B **113**, 8210 (2009).

[34] K. E. Furse and S. A. Corcelli, J. Phys. Chem. Lett. **1**, 1813 (2010).

[35] M. A. Berg, R. S. Colemanb, and C. J. Murphy, Phys. Chem. Chem. Phys. **10**, 1229 (2008).

[36] B. Bagchi and B. Jana, Chem. Soc. Rev. **39**, 1936 (2010).

[37] E. B. Brauns, M. L. Madaras, R. S. Coleman, C. J. Murphy, and M. A. Berg, J. Am. Chem. Soc. **121**, 11644 (1999).

[38] R. J. Cave and E. W. Castner, J. Phys. Chem. A **106**, 12117 (2002).

[39] I. S. Joung and T. E. Cheatham, J. Phys. Chem. B **112**, 9020 (2008).

[40] W. D. Cornell, P. Cieplak, C. I. Bayly, I. R. Gould, K. M. Merz, D. M. Ferguson, D. C. Spellmeyer, T. Fox, J. W. Caldwell, and P. A. Kollman, J. Am. Chem. Soc. **117**, 5179 (1995).

[41] J. Wang, P. Cieplak, and P. A. Kollman, J. Comput. Chem. **21**, 1049 (2000).

[42] A. Perez, I. Marchan, D. Svozil, J. Sponer, T. E. Cheatham, C. A. Laughton, and M. Orozco, Biophys. J. **92**, 3817 (2007).

[43] M. Zgarbova, F. J. Luque, J. Sponer, T. E. Cheatham, M. Otyepka, and P. Jurecka, J. Chem. Theory Comput. **9**, 2339 (2013).

[44] H. J. C. Berendsen, J. R. Grigera, and T. P. Straatsma, J. Phys. Chem. **91**, 6269 (1987).

[45] C. I. Bayly, P. Cieplak, W. D. Cornell, and P. A. Kollman, J. Phys. Chem. **97**, 10269 (1993).

[46] W. D. Cornell, P. Cieplak, C. I. Bayly, and P. A. Kollman, J. Am. Chem. Soc. **115**, 9620 (1993).

[47] U. Essmann, L. Perera, M. L. Berkowitz, T. Darden, H. Lee, and L. G. Pedersen, J. Chem. Phys. **103**, 8577 (1995).

[48] A. K. Mazur, J. Am. Chem. Soc. **120**, 10928 (1998).

[49] H. J. C. Berendsen, J. P. M. Postma, W. F. van Gunsteren, A. DiNola, and J. R. Haak, J. Chem. Phys. **81**, 3684 (1984).

[50] A. K. Mazur, J. Comput. Chem. **18**, 1354 (1997).

[51] A. K. Mazur, J. Chem. Phys. **111**, 1407 (1999).

[52] A. K. Mazur, J. Phys. Chem. B **102**, 473 (1998).

[53] A. K. Mazur, Biophys. J. **91**, 4507 (2006).

[54] A. K. Mazur, J. Chem. Theory Comput. **5**, 2149 (2009).